

## Flavonoidal glycosides and *in vitro* antioxidant activity of *Bignonia binata* Thunb. leaves Family Bignoniaceae and *in silico* evidence of their potential anti-COVID-19 activity

Ashraf N.E. Hamed<sup>1\*#</sup>, Mamdouh N. Samy<sup>1#</sup>, Basma K. Mahmoud<sup>1</sup>, Eman Z. Attia<sup>1</sup>, Taha F.S. Ali<sup>2</sup>, Ahmed H. Afifi<sup>3</sup>, Mohamed S. Kamel<sup>1,4</sup>

<sup>1</sup>Department of Pharmacognosy, Faculty of Pharmacy, Minia University, 61519 Minia, Egypt.

<sup>2</sup>Department of Medicinal Chemistry, Faculty of Pharmacy, Minia University, 61519 Minia, Egypt.

<sup>3</sup>Division of Pharmaceutical Industries, Department of Pharmacognosy, National Research Center, 12622, Dokki, Giza, Egypt.

<sup>4</sup>Department of Pharmacognosy, Faculty of Pharmacy, Deraya University, 61111 New Minia, Egypt.

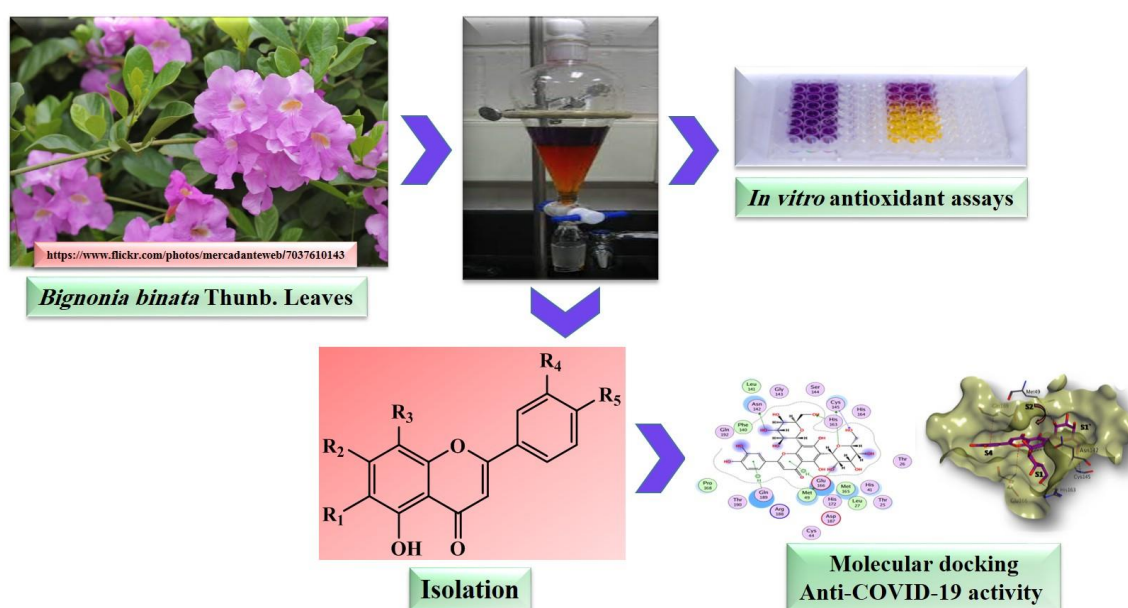
Received: January 30, 2021; revised: March 16, 2021; accepted: March 16, 2021

### Abstract

One *O*- and three *C*-flavonoidal glycosides were isolated from the EtOAc and aqueous fractions of the total ethanolic extract of *Bignonia binata* Thunb. leaves (TEEBB). The structure elucidation of the compounds was based on both 1D and 2D NMR spectroscopic experimental analyses and ESI-MS, as well as by comparison with the literature. They were identified as chrysoeriol 7-*O*- $\beta$ -D-glucopyranoside (**1**), apigenin-6,8-di-*C*- $\beta$ -D-glucopyranoside (**2**), luteolin 6,8-di-*C*- $\beta$ -D-glucopyranoside (**3**) and apigenin 6-*C*- $\alpha$ -L-arabinopyranosyl-8-*C*- $\beta$ -D-glucopyranoside (**4**). Whereas, compounds **1** and **3** were isolated for the first time from the family Bignoniaceae and compound **4** for the first time from *Bignonia* genus. Additionally, the antioxidant potency evaluation of the TEEBB and different fractions revealed the high potency of the 50% MeOH sub-fraction of the aqueous fraction (50%MAqF) as DPPH radical scavenger, followed by the EtOAc fraction. Likewise, the highest antioxidant capacity was obtained by the EtOAc fraction and 50%MAqF in phosphomolybdate assay. Molecular docking simulation of the isolated flavonoidal glycosides to SARS-CoV-2 Mpro revealed their high binding affinity and their therapeutic potential against COVID-19.

### Key words

*Bignonia binata* (*Clytostoma binatum*); Antioxidant; Flavonoids; Molecular docking; COVID-19; SARS-CoV-2.



\* Correspondence: Ashraf N. E. Hamed

Tel.: +2086-234-77-59; Fax: +2086-236-90-75.

Email Address: [ashrafnag@mu.edu.eg](mailto:ashrafnag@mu.edu.eg)

#These authors are equally contributing this work.

## 1. Introduction

Since the first unveiling of the novel coronavirus (2019-nCoV, or COVID-19) in Wuhan, China in December 2019, unprecedented dares presented by the rapidly rising COVID-19 pandemic health crisis are confronting people all over the globe. COVID-19, a single-stranded RNA virus is complicated by severe acute respiratory syndrome coronavirus 2 (SARS-CoV-2), a newly identified virus alike SARS-CoV and MERS-CoV-2 that cause the severe acute respiratory syndrome and the Middle East respiratory syndrome respectively [1].

Polyphenols are an enormous family of more than 10,000 naturally occurring secondary metabolites, which have unlimited pharmacological activities for human health as many chronic diseases such as neurological, cardiovascular diseases, diabetes and cancer. Various studies and clinical trials progressively proved the role of polyphenols in controlling numerous human pathogens including MERS and SARS, which are quite like to COVID-19 by increasing immune response against viral infections by diverse biological mechanisms viz., quercetin, rutin, resveratrol, kaempferol, apigenin, luteolin, genistein, naringenin, daidzein, chrysin, hesperetin, galangin, eriodictyol, neobavaisoflavone and catechin [2].

Bignoniaceae (Bignoniaceae), with 31 lianas species distributed from Argentina to USA. *Bignonia* L. is the fifth largest genus in Bignoniaceae [3,4]. Numerous species were reported to have various phytoconstituents belonging to various chemical classes e.g. flavonoids, iridoids, quinones, xanthenes, lignans, coumarins, sterols, diterpenes, triterpenes, saturated and unsaturated fatty acids,...etc [5]. The species of genus *Bignonia* are reported to be used as anti-diabetic, wound healing, protection against light, gastric protection, hepatic renal and heart protection, anti-obesity, male fertility, sleep induction, cytotoxic, antioxidant, anti-inflammatory, antimicrobial activities,...etc [5].

*Bignonia binata* Thunb. (syn: *Clytostoma binatum* Thunb.) is distributed from Mexico to Argentina [3]. Ten compounds were formerly isolated, which are belonging to phenolics, sterols, triterpenes, nitrogenous compounds and iridoids. Besides, the DPPH radical scavenging, cytotoxic, antimicrobial, antimalarial, antitypanosomal, hepatoprotective and nephroprotective activities were previously reported [6-8]. Additionally, the chemical profile was investigated by LC-HR-ESI-MS, where it revealed the presence of twelve compounds related to phenylethanoids, flavonoidal glycosides and iridoids [8]. Furthermore, the EtOAc fraction and total ethanolic extract of *B. binata* Thunb. exhibited the highest amount of total phenolic and flavonoidal contents, respectively [8]. The newly emerging ailments such as the novel COVID-19 and other infectious diseases, which make serious complications on both human health and economy worldwide, need crucial research for discovering a new antiviral drug preferably from a natural source such as polyphenols [9,10]. The above-mentioned data encouraged us to carry out a phytochemical study to isolate the phenolic compounds from the polar fractions of the total ethanolic extract of *B. binata* leaves in addition to in silico modeling study of these isolated compounds against SARS-CoV-2 Mpro.

## 2. Materials and Methods

### 2.1. Plant material

*Bignonia binata* leaves were collected from El-Zohria Botanical Garden, Giza, Egypt on 15/12/2015. The plant was identified by Mr. Ahmed Shokry, Director of El-Zohria Botanical Garden and confirmed by Prof. Dr. Barkat N., Botany Department, Faculty of Science, Minia University. The voucher specimen was deposited in the Herbarium of Pharmacognosy Department, Faculty of Pharmacy, Minia University, Minia, Egypt under registration number (Mn-ph-Cog-033).

### 2.2. Chemicals

Solvents and chemicals [light petroleum ether (60-80 °C), dichloromethane (DCM), ethyl acetate (EtOAc), methanol, ethanol, glacial acetic acid (HAc), H<sub>2</sub>SO<sub>4</sub>,  $\alpha$ -naphthol, potassium hydroxide (KOH) and ammonia (NH<sub>3</sub>)] were obtained from El-Nasr Company, for Pharmaceuticals and Chemicals, Egypt. Acetonitrile (CH<sub>3</sub>CN) and methanol of HPLC grade were obtained from SDFCL sd fine-Chem Limited, India. The deuterated solvent used for NMR spectroscopic analyses dimethyl sulfoxide (DMSO-*d*<sub>6</sub>) was purchased from (Sigma-Aldrich, Germany).

### 2.3. Equipments

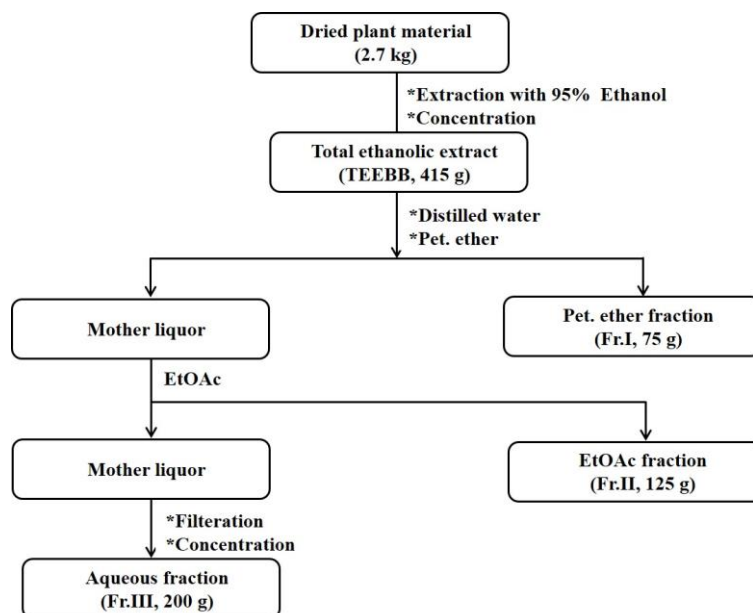
Portable UV-lamp with short and long wavelength for localization of the fluorescent spots, (USA), BRUKER (400 and 500 MHz spectrometer, Germany), LTQ Orbitrap XL mass spectrometer used for ESI-MS (Japan), HPLC KNAUER Agilent Technologies Series 1100 [Smartline S-2600 UV-VIS multiwavelength detector coupled with Smartline S-1000 quaternary pump, Knauer dynamic mixing chamber, ALS] (UV Detect00719, Knauer, Berlin, Germany).

### 2.4. HPLC instrumental conditions

The Knauer HPLC equipment was used. The separation was carried out on Phenomenex C18 (4.6 x 250 mm, 10  $\mu$ m, Phenomenex, Bondo ione, USA), reversed phase column, utilized with guard column filled with the same stationary phase. The mobile phase was composed of deionized H<sub>2</sub>O (containing 0.1% glacial HAc), CH<sub>3</sub>CN and MeOH (HPLC grade), using gradient elution system. The mobile phase was filtered under vacuum through (a 0.45  $\mu$ m membrane filter) and degassed. The chromatograms were processed using a Eurochrom for windows program (Basic ed. V3.05, Advanced Scientific Instruments Wissenschaftliche Geraetebau, Germany). Compounds (2-3) were eluted with a solvent system (deionized H<sub>2</sub>O-CH<sub>3</sub>CN-MeOH) gradient elution with decreasing the polarity, starting with a concentration of deionized H<sub>2</sub>O-CH<sub>3</sub>CN-MeOH (90:9:1) and increasing the concentration of CH<sub>3</sub>CN-MeOH, while deionized H<sub>2</sub>O was decreased linearly within 50 min up to deionized H<sub>2</sub>O-CH<sub>3</sub>CN-MeOH (40:54:6) with flow rate 2 mL/min.

### 2.5. Extraction, fractionation and isolation of the constituents

The air-dried powdered leaves of *B. binata* (2.7 kg) were extracted by maceration with 95% ethanol till exhaustion. The total ethanolic extract (TEEBB) was concentrated under reduced pressure to obtain a viscous dark green residue (415 g). TEEBB was suspended in 400 mL of distilled water, transferred to a separating funnel and defatted with successive portions of petroleum ether (300 mL, each 6x). The combined petroleum ether fractions were concentrated under reduced pressure to yield fraction (Fr.I, 75 g). The mother liquor was repartitioned with successive portions of EtOAc (300 mL each, x6). The combined EtOAc fractions were concentrated under reduced pressure to yield fraction (Fr.II, 125 g). Finally, the remaining mother liquor (aqueous fraction) was concentrated under reduced pressure to afford fraction (Fr.III, 200 g).



Scheme 1: Fractionation of the TEEBB.

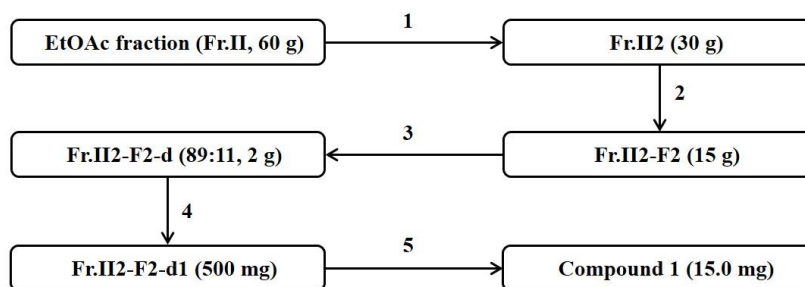


## Chart key:

- 1-Silica VLC, EtOAc-MeOH Gr. Elu., 4 Subfractions.
- 2-Silica gel CC, EtOAc-MeOH, Gr. Elu., 5 Subfractions.
- 3-Silica gel VLC, DCM-MeOH Gr. Elu., 8 Subfractions.
- 4-Sephadex LH-20 CC, MeOH, 2 Subfractions.
- 5-Sephadex LH-20 CC, MeOH, Followed by preparative TLC Silica gel, DCM-MeOH, 95:5.

Scheme 2: Isolation of compound 1.

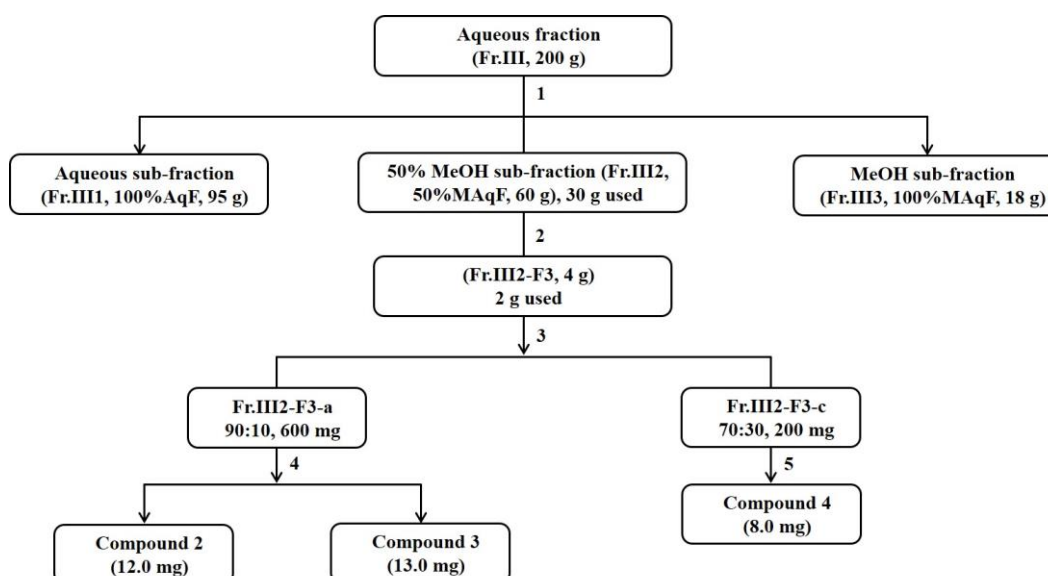


## Chart key:

- 1-Diaion HP-20, H<sub>2</sub>O, 50% MeOH, 100% MeOH, 3 Subfractions.
- 2-Silica gel VLC, EtOAc-MeOH, Gr. Elu., 5 Subfractions.
- 3-RP<sub>18</sub>, H<sub>2</sub>O-MeOH, Gr. Elu., 4 Subfractions.
- 4-Sephadex LH-20 CC, H<sub>2</sub>O-MeOH (70:30) followed by HPLC.
- 5-Sephadex LH-20 CC, H<sub>2</sub>O-MeOH (70:30).

Scheme 3: Isolation of compounds (2-4).

The fractionation process of TEEBB is summarized in Scheme 1.

The EtOAc fraction (II) was divided into two equivalent parts (each 60 g). Both of them were subjected to fractionation using VLC-technique. Elution was performed initially using EtOAc and then EtOAc-MeOH gradient mixtures in order of increasing the polarity gradually in 10% by MeOH till EtOAc-MeOH (70:30). The effluents were collected in fractions (3 L each). Each polarity was concentrated under reduced pressure affording 4 sub-fractions (Fr.II1-Fr.II4). Sub-fraction (Fr.II2, 30 g) was further fractionated on silica gel CC (77 x 6 cm), using EtOAc-MeOH gradient mixtures to give five sub-fractions Fr.II2-F1:Fr.II2-F5. Fr.II2-F2 (15 g) was rechromatographed on silica gel VLC (40 x 4 cm) gradient elution with DCM-MeOH, affording eight sub-fractions Fr.II2-F2-a:Fr.II2-F2-h. Sub-fraction (Fr.II2-F2-d, 2.0 g) was obtained from elution system DCM-MeOH (89:11). It was chromatographed on sephadex LH-20 CC using MeOH, giving 2 sub-fractions Fr.II2-F2-d1 and Fr.II2-F2-d2. Sub-fraction Fr.II2-F2-d1 (500 mg) was rechromatographed on sephadex LH-20 CC using MeOH followed by preparative TLC silica gel. It was developed with DCM-MeOH (95:5) to yield compound **1** (15.0 mg). The chromatographic isolation of compound **1** is summarized in Scheme 2.

The aqueous fraction was applied to the top of the Diaion HP-20 column chromatography. It was eluted with H<sub>2</sub>O, 50% MeOH and MeOH (300 mL each, x6) in the order of decreasing polarities, affording 3 sub-fractions; aqueous sub-fraction (Fr.III1, 100%AqF, 95 g), 50% MeOH sub-fraction (Fr.III2, 50%MAqF, 60 g) and MeOH sub-fraction (Fr.III3, 100%MAqF, 18 g). Only (30 g) of the sub-fraction Fr.III2 (50%MAqF, 60 g) was submitted to further fractionation using VLC technique, which eluted firstly with EtOAc-MeOH (90:10) and then increasing the polarity 20% till EtOAc-MeOH and finally MeOH. The effluents were collected in fractions (3 L each). Each polarity was concentrated under reduced pressure affording five sub-fractions Fr.III2-F1:Fr.III2-F5. Fr.III2-F3 (2.0 g) was rechromatographed on a RP18 CC H<sub>2</sub>O-MeOH gradient elution to give four sub-fractions Fr.III2-F3-a:Fr.III2-F3-d. The subtraction Fr.III2-F3-a (600 mg) was rechromatographed on a sephadex LH-20 CC using H<sub>2</sub>O-MeOH (70:30) and then subjected to HPLC purification, using H<sub>2</sub>O-CH<sub>3</sub>CN-MeOH gradient elution to afford compounds; **2** (12.0 mg; Rt= 18.59) and **3** (13.0 mg; Rt= 17.40), while sub-fraction (Fr.III2-F3-c, 200 mg) was subjected to a sephadex LH-20 CC using H<sub>2</sub>O-MeOH (70:30), yielding compounds **4** (8.0 mg). The chromatographic isolation of compounds (**2-4**) is summarized in Scheme 3.

## 2.6. *In vitro* antioxidant assays

Each sample was dissolved in methanol (95%) to provide a concentration of 2.5 mg/mL and then made serial dilution to prepare suitable concentrations for antioxidant assays.

### 2.6.1. DPPH assay

The free radical scavenging activity of the TEEBB and its derived different fractions was estimated spectrophotometrically using 2,2-diphenyl-1-picryl-hydrazyl (DPPH). In brief, 200  $\mu$ L of each sample (at various concentrations) was added to 2 mL of DPPH solution (0.1 mM), the mixture was well shaken and kept in the dark at 25 °C, for 15 min. We prepared the control by using MeOH instead of the sample and the absorbance was measured (3 times) at 517 nm. The concentration, which

reduced half of the initial DPPH<sup>-</sup> concentration (EC<sub>50</sub>) was calculated from the graph of DPPH scavenging effect against sample concentration [11].

### 2.6.2. Phosphomolybdate assay

The total reducing abilities of the TEEBB and its derived different fractions were assessed by phosphomolybdate complex method, in which the ascorbic acid was used as a standard. Briefly, 0.3 mL of sample solution (2.5 mg/mL) was mixed with 3 mL of reagent solution (0.6 M sulphuric acid, 28 mM sodium phosphate and 4 mM ammonium molybdate) in capped tubes, which were incubated in a water bath for 90 min at 95 °C. After cooling, the absorbance was measured at 695 nm against a blank (3 times). The calibration curve was made using ascorbic acid, so that the antioxidant activity was expressed in mg ascorbic acid equiv./g dried sample [11].

## 2.7. Molecular docking

Docking study was achieved using Molecular Operating Environment (MOE) 2019.01 software (Chemical Computing Group, Montreal, QC, Canada). The X-ray co-crystal structure of SARS-CoV-2 complexed with N3 inhibitor (PDB code: 7BQY) [12] was downloaded from Protein Data Bank. In the preparation section, the MOE QuickPrep protocol was employed to correct structural issues, protonate, delete water molecules, tether atoms and minimize the protein structure. 2D structures of the ligands were sketched using ChemBioDraw Ultra 14.0 software (Cambridge Soft corporation). The ligands were minimized by MMFF94x Force Field with the default setting. Docking calculations were performed using the induced fit method, where the co-crystallized ligand N3 was considered the center of the docking site. All other docking parameters such as the force field and the number of the docking poses were kept MOE default settings. The generated docking poses were ranked according to their docking scores and the best energy pose was selected.

## 2.7. Statistical analyses

Data are presented as mean $\pm$ SEM and was determined by one-way analysis of variance (ANOVA) test followed by Dunnett test. Statistically significant differences \*( $p < 0.05$ ), \*\*( $p < 0.01$ ), \*\*\*( $p < 0.001$ ), relative to TEEBB of each sample using the Graph Pad Prism 6 software (Version 6.00 for Windows, GraphPad Software, San Diego California USA, www.graphpad.com).

## 3. Results and discussion

### 3.1. Phytochemical study

All compounds were isolated as yellow powders. They exhibited brown fluorescence under UV lamp (365 nm) and yellow color after spraying with 10% v/v H<sub>2</sub>SO<sub>4</sub> reagent. They gave a positive color reaction with Molisch's test indicating its glycosidal nature and yellow color with (KOH & NH<sub>3</sub>) indicating its flavonoidal nature.

**Compound 1** demonstrated R<sub>f</sub> = 0.5 on normal phase silica gel TLC plate using system DCM-MeOH (86:14). The negative ESI-MS spectrum showed fragment at  $m/z$  461.4 [M-H]<sup>-</sup> calculated to the molecular formula C<sub>22</sub>H<sub>22</sub>O<sub>11</sub>. By comparing the <sup>1</sup>H-NMR (400 MHz, DMSO-*d*<sub>6</sub>),

**Table 1:** <sup>1</sup>H-NMR spectral data of the isolated compounds (1-4).

No.	$\delta_H$ (Integration, Multiplicity, <i>J</i> in Hz)			
	(1)	(2)	(3)	(4)
H-3	6.96 (1H, s)	6.80 (1H, s)	6.69 (1H, s)	6.90 (1H, s)
H-6	6.45 (1H, d, 2.04)			
H-8	6.67 (1H, d, 2.04)			
H-2'			7.48 (1H, br s)	
H-5'			6.88 (1H, d, 8.4)	
H-6'			7.55 (1H, br d, 8.4)	
H-2',6'	7.60 (2H, overlapped)	8.03 (2H, d, 8.1)		8.04 (2H, d, 6.5)
H-3',5'		6.90 (2H, d, 8.1)		6.92 (2H, d, 6.5)
H-5'	6.93 (1H, d, 8.44)			
OCH <sub>3</sub> -3'	3.88 (3H, s)			
H-1''	5.07 (1H, d, 7.36)	4.77 (1H, d, 10)	4.76 (1H, d, 9.8)	4.72 (1H, d, 9.1)
H-1'''		4.80 (1H, d, 9.9)	4.81 (1H, d, 9.6)	4.79 (1H, d, 8.4)

(DMSO-*d*<sub>6</sub>, 400 MHz).**Table 2:** <sup>13</sup>C-NMR spectral data of the isolated compounds (1-4).

No.	$\delta_C$ (Multiplicity)			
	(1)	(2)	(3)	(4)
C-2	164.3 (s)	163.9 (s)	164.2 (s)	163.6 (s)
C-3	103.1 (d)	102.5 (d)	102.5 (d)	102.2 (d)
C-4	182.0 (s)	182.2 (s)	182.2 (s)	181.9 (s)
C-5	161.1 (s)	158.7 (s)	158.6 (s)	157.9 (s)
C-6	99.5 (d)	107.6 (s)	107.5 (s)	107.8 (s)
C-7	162.9 (s)	161.2 (s)	163.7 (s)	161.5 (s)
C-8	95.0 (d)	105.3 (s)	105.2 (s)	104.8 (s)
C-9	156.9 (s)	155.1 (s)	155.1 (s)	154.8 (s)
C-10	105.3 (s)	103.5 (s)	103.8 (s)	103.2 (s)
C-1'	121.9 (s)	121.5 (s)	121.5 (s)	121.2 (s)
C-2'	110.3 (d)	129.0 (d)	114.1 (d)	128.7 (d)
C-3'	148.3 (s)	115.8 (d)	145.8 (s)	115.5 (d)
C-4'	150.7 (s)	161.2 (s)	149.7 (s)	161.0 (s)
C-5'	116.0 (d)	115.8 (d)	115.6 (d)	115.5 (d)
C-6'	120.7 (d)	129.0 (d)	119.4 (d)	128.7 (d)
OCH <sub>3</sub> -3'	55.9 (q)			
C-1''	100.0 (d)	73.4 (d)	73.4 (d)	73.9 (d)
C-2''	73.1 (d)	71.0 (d)	70.8 (d)	68.1 (d)
C-3''	76.5 (d)	77.9 (d)	77.8 (d)	73.9 (d)
C-4''	69.6 (d)	70.6 (d)	70.7 (d)	69.2 (d)
C-5''	77.3 (d)	81.9 (d)	82.1 (d)	69.8 (t)
C-6''	60.6 (d)	59.9 (t)	59.8 (t)	
C-1'''		74.1 (d)	74.1 (d)	73.6 (d)
C-2'''		71.8 (d)	71.9 (d)	70.6 (d)
C-3'''		78.9 (d)	78.9 (d)	78.5 (d)
C-4'''		69.1 (d)	69.1 (d)	70.2 (d)
C-5'''		80.9 (d)	80.9 (d)	81.6 (d)
C-6'''		61.3 (t)	61.6 (t)	60.9 (t)

(DMSO-*d*<sub>6</sub>, 100 MHz)**Table 3:** Antioxidant assays of TEEBB and its derived different fractions.

Sample	Method	EC <sub>50</sub> for DPPH radical scavenging assay	Phosphomolybdate assay (mg Ascorbic equiv./g dried sample)
		TEEBB	109.9±0.02
Petroleum ether fraction	101.7±0.04***	16.5±0.37***	
EtOAc fraction	71.3±0.02***	68.8±0.76***	
Aqueous fraction	111.7±0.06***	20.3±0.44***	
50%MAqF	14.3±0.12***	59.6±1.16***	
100%MAqF	86.5±0.06***	30.5±0.45*	

EC<sub>50</sub> is µg/mL. Each value represented as mean±SEM (n=3) Statistically significant differences \*(*p*<0.05), \*\*(*p*<0.01), \*\*\*(*p*<0.001), relative to TEE of each plant according to Dunnett's multiple comparison test.

APT (100 MHz, DMSO-*d*<sub>6</sub>) and HMBC spectral data, which are displayed in Figure 1 and Tables 1 & 2 with the literature [13], it was identified as chrysoeriol 7-*O*- $\beta$ -D-glucopyranoside (syn.: termopsoside or thermopsoside). It is reported for the first time in the family Bignoniaceae.

**Compound 2** demonstrated  $R_f = 0.3$  on RP<sub>18</sub> TLC plate using system DCM-MeOH (60:40). The negative ESI-MS spectrum showed fragment at  $m/z$  593.3 [M-H]<sup>-</sup> calculated to the molecular formula C<sub>27</sub>H<sub>30</sub>O<sub>15</sub>. It was identified as apigenin-6,8-di-*C*- $\beta$ -D-glucopyranoside (syn.: vicenin-2) through the comparison of the <sup>1</sup>H-NMR (500 MHz, DMSO-*d*<sub>6</sub>), APT (125 MHz, DMSO-*d*<sub>6</sub>) and HMBC spectral data are displayed in Figure 1 and Tables 1 & 2 with the literature [14-15]. It is also reported for the first time in the family Bignoniaceae. This represents the first report for separation of this compound from the *B. binata*, whereas previously isolated from *Macfadyena unguis-cati* [16-17].

**Compound 3** demonstrated  $R_f = 0.35$  on RP<sub>18</sub> TLC plate using system DCM-MeOH (60:40). The negative ESI-MS spectrum showed fragment at  $m/z$  609.5 [M-H]<sup>-</sup> consistent with the molecular formula C<sub>27</sub>H<sub>30</sub>O<sub>16</sub>. The <sup>1</sup>H-NMR (500 MHz, DMSO-*d*<sub>6</sub>) and APT (125 MHz, DMSO-*d*<sub>6</sub>) spectral data are illustrated in Figure 1 and Tables 1 & 2 were compared with the literature [18-19], resulted in the identification of compound **3** as luteolin 6,8-di-*C*- $\beta$ -D-glucopyranoside (syn.: lucenin-2). It is reported for the first time in the family Bignoniaceae.

**Compound 4** demonstrated  $R_f = 0.2$  on RP<sub>18</sub> TLC plate using system DCM-MeOH (60:40). The negative ESI-MS spectrum showed fragment at  $m/z$  563.2 [M-H]<sup>-</sup> calculated to the molecular formula C<sub>26</sub>H<sub>28</sub>O<sub>14</sub>. In comparison with the literature [20-21], it was identified as apigenin 6-*C*- $\alpha$ -L-arabinopyranosyl-8-*C*- $\beta$ -D-glucopyranoside (syn.: isoschaftoside). The <sup>1</sup>H-NMR (400 MHz, DMSO-*d*<sub>6</sub>), DEPT-Q (100 MHz, DMSO-*d*<sub>6</sub>) and HMBC spectral data are displayed in Figure 1 and Tables 1 & 2. It is the first report for isolation of this compound from genus Bignonia.

### 3.2. Antioxidant

The TEEBB and its derived different fractions demonstrated potent radical scavenging activity, in which the 50%MAqF is the most effective DPPH radical scavenger sample, having the least EC<sub>50</sub> = 14.3±0.12 µg/mL followed by the EtOAc fraction with EC<sub>50</sub> = 71.3±0.02 µg/mL. Also, in phosphomolybdate assay, the highest antioxidant capacity was obtained by the EtOAc fraction and 50%MAqF with 68.8±0.76 and 59.6±1.16 mg ascorbic acid equiv./g dried sample, respectively. Both the antioxidant activities, indicating the strong relationship between the presence of phenolics and the free radical scavenging activity, in which these samples exhibited high phenolic content and had also a potent radical scavenging activity [8]. All antioxidant results are shown in Table 3.

### 3.3. Molecular docking

The pandemic COVID-19 disease caused SARS-CoV-2 virus represents a significant challenge for drug discovery efforts [22]. The main protease (Mpro or 3CL pro) is an essential enzyme for SARS-CoV-2 survival. It is responsible for processing viral non-structural proteins; hence, it is considered a potential target for developing and discovering effective

antiviral drugs [23]. Plant flavonoids such as rutin, morin, quercetin, apigenin, hesperidin and catechin have been reported to possess antiviral activity against a broad spectrum of viruses [24]. Several flavonoids have demonstrated inhibitory activity against 3CL pro, such as hesperetin (IC<sub>50</sub> = 60 µM), hyperoside (IC<sub>50</sub> = 42.79 µM) and GCG (IC<sub>50</sub> = 47 µM) [25-26]. In this study, *in silico* approach has been used to predict the binding affinity and activity of the isolated compound as SARS-CoV-2 Mpro inhibitors.

The top-ranked poses for the isolated compounds and N3 inhibitor docked to the binding pocket of SARS-CoV-2 Mpro (PDB code: 7BQY) are displayed in Figure 2. In contrast, the docking score ( $\Delta G$ ) of all ligands and their H-bond interaction to binding pocket residues are summarized in Table 4. As shown in Figure 3, among the isolated compounds, the three flavone-6,8-*C*-diglycosides (**2-4**) have occupied the four substrate-binding pocket subsites (S1, S2, S4 and S1') as well as the N3 inhibitor. In contrast, termopsoside (**1**), a 7-*O*-glucosylated flavone, has occupied only three subsites (S2, S4 and S1'). As compiled in Table 4, all the isolated compounds have demonstrated a binding affinity superior to hyperoside. Lucenin-2 (**3**) and vicenin-2 (**2**) have shown the best docking score (-10.387 and -10.065 respectively), followed by isoschaftoside (**4**) (-9.515) and at last termopsoside (**1**) (-8.696). The superior affinity of the three flavone-*C*-diglycosides over the flavonoid-*O*-monoglycosides to the substrate-binding pocket of SARS-CoV-2 Mpro could be explained by the ability to form more interactions with the binding site key amino acids. According to the above results, compounds **2**, **3** and **4** could be considered potential candidates as SARS-CoV-2 Mpro inhibitors and hyperoside was used as a structurally related inhibitor for comparison.

### 4. Conclusion


Due to the reported *C*-flavonoidal glycosides of *B. binata* Thunb. leaves, in addition to their promising affinity toward SARS-CoV-2 Mpro as demonstrated by docking study, they could be considered as potential candidates against COVID-19. Therefore, further investigations could have a supportive role in the pharmaceutical field towards the development of new anti-COVID-19 drugs.

### Conflict of interest

The authors declare that there is no conflict of interest regarding these studies.

### Orcid

Ashraf N. E. Hamed  [orcid.org/0000-0003-2230-9909](https://orcid.org/0000-0003-2230-9909)

Mamdouh N. Samy  [orcid.org/0000-0002-2128-5389](https://orcid.org/0000-0002-2128-5389)

Taha F. S. Ali  [orcid.org/0000-0002-8881-0408](https://orcid.org/0000-0002-8881-0408)

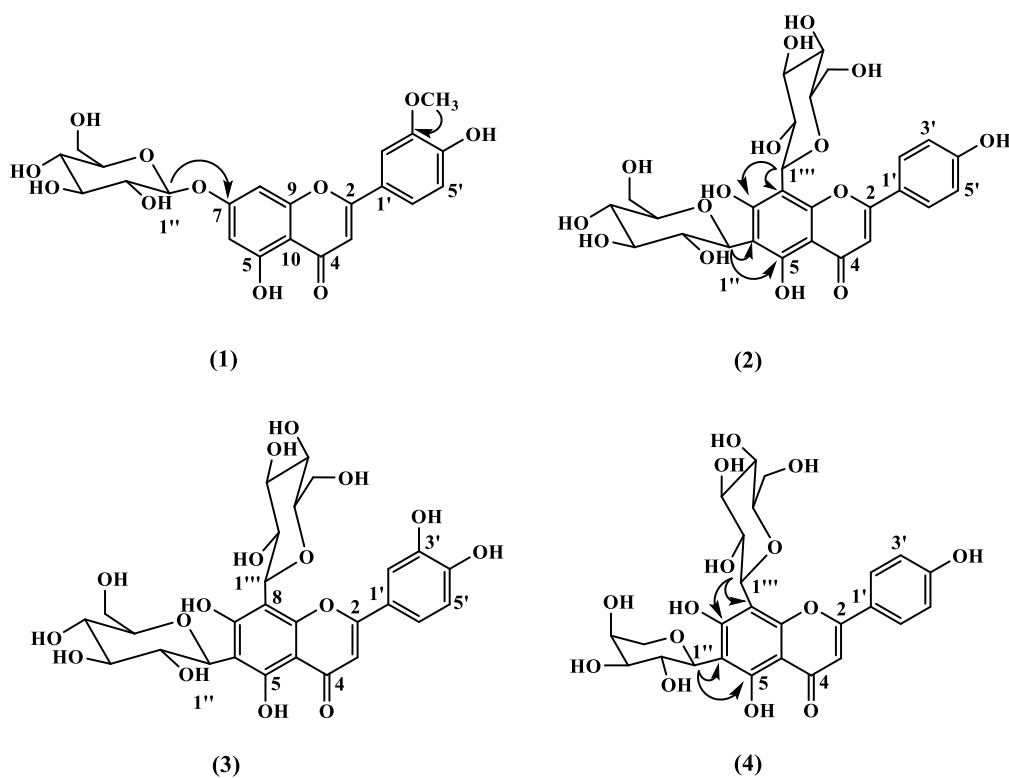


**Figure 1:** The chemical structures with significant HMBC correlations ( $^1\text{H} \rightarrow ^{13}\text{C}$ ) of the isolated compounds (1-4).

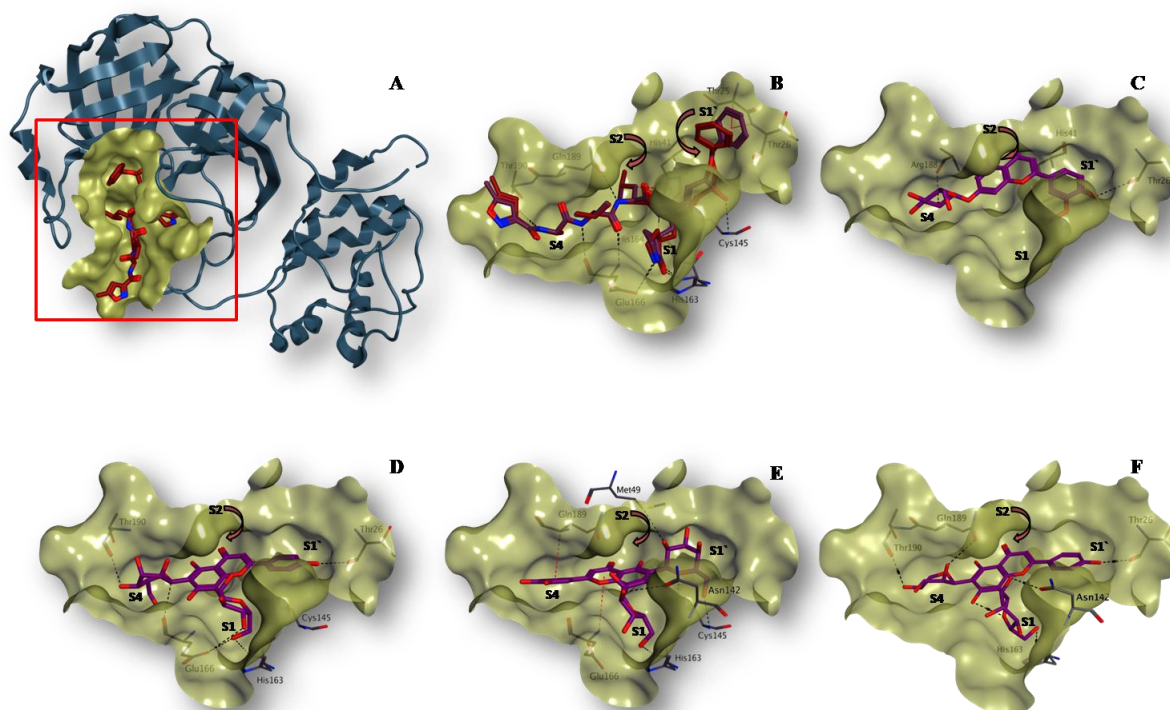


**Figure 2:** SARS-CoV-2 Mpro binding modes for inhibitor N3 and the isolated compounds (1-4). (A) Cartoon presentation of single protomer of SARS-CoV-2 Mpro (Blue ribbons, PDB code: 7BQY) with substrate-binding pocket (gold surface) in complex with the inhibitor N3 (red sticks). (B) Superposition of co-crystallized (red) and docked (magenta) N3 inhibitor in the Mpro binding pocket. (C-F) Docking poses of the isolated compounds (1-4) in Mpro binding pocket.

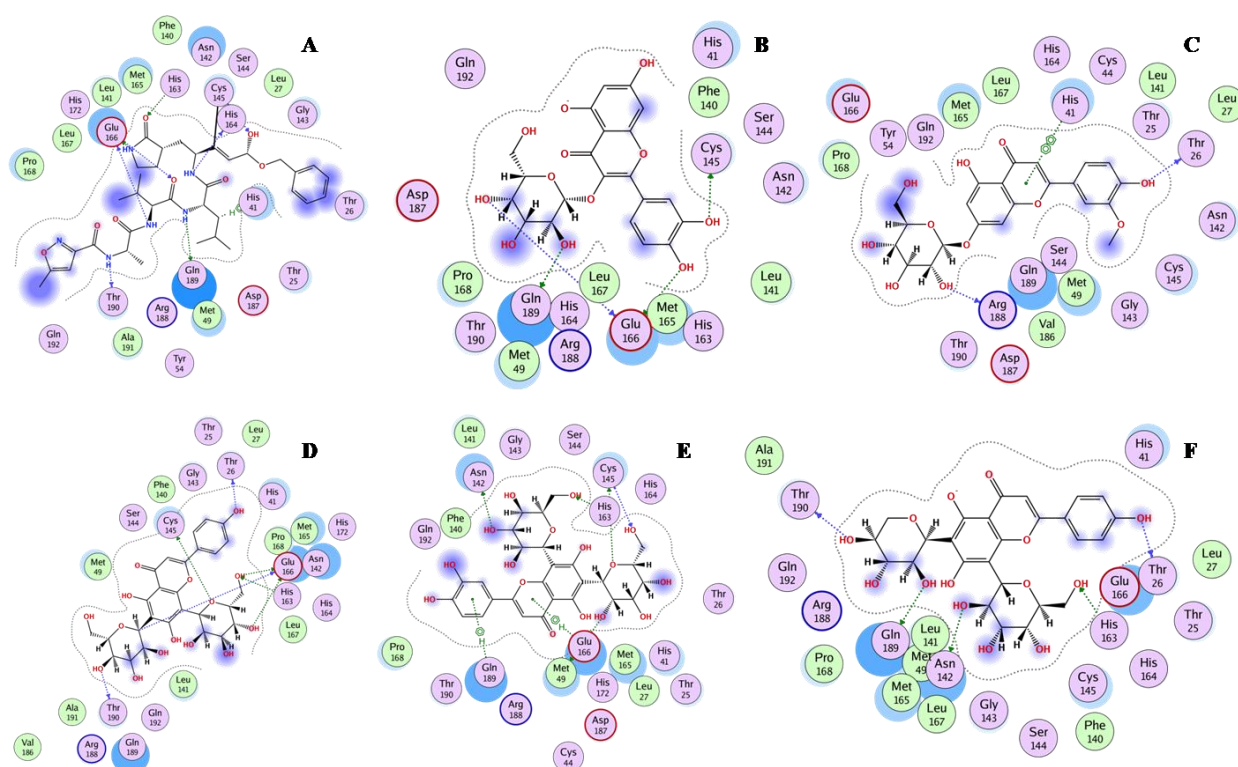


**Figure 3:** 2D presentation of the binding interaction between the isolated compounds and the critical amino acids in the active site of SARS-CoV-2 Mpro compared to co-crystallized N3 inhibitor and the structurally related inhibitor Hyperoside. (A) N3 inhibitor, (B) Hyperoside and (C-F) Isolated compounds (1-4).

**Table 4:** Docking results of the isolated compounds (1-4) with the active site of SARS-CoV-2 Mpro compared to a structurally related inhibitor (Hyperoside).

No.	Ligand		Binding affinity ( $\Delta G$ in Kcal/mol)	Hydrogen-bonds parameters	
				AA Residue	$\delta$ ( $\text{\AA}$ )
	N3		-12.209	CYS145 (Backbone NH)	3.64
				HIS163 (Imidazole)	1.94
				GLU166 (Side chain COOH)	1.96
				GLU166 (Backbone NH)	1.96
				GLU166 (Backbone CO)	2.29
				GLN189 (Side chain CONH <sub>2</sub> )	1.96
				THR190 (Backbone CO)	2.40
	Hyperoside		-8.467	CYS 145 (Side chain SH)	2.54
				GLU166 (Backbone CO)	2.05
				GLU166 (Side chain COOH)	2.24
				GLN189 (Side chain CONH <sub>2</sub> )	2.13
1	Chrysoeriol	7-O- $\beta$ -D-	-8.696	THR26 (Backbone CO)	2.12
	glucopyranoside			ARG188 (Backbone CO)	1.94
2	Apigenin-6,8-di-C- $\beta$ -D-		-10.065	THR26 (Backbone CO)	2.13
	glucopyranoside			HIS163 (Imidazole)	2.30
				GLU166 (Side chain COOH)	2.50
				GLU166 (Side chain COOH)	2.47
				GLU166 (Backbone CO)	2.28
				THR190 (Backbone CO)	2.03
3	Luteolin	6,8-di-C- $\beta$ -D-	-10.387	MET 49 (Side chain SCH <sub>3</sub> )	3.32
	glucopyranoside			ASN142 (Side chain COOH)	2.27
				CYS145 (Side chain SH)	3.25
				CYS145 (Backbone NH)	2.12
				HIS163 (Imidazole)	2.12
4	Apigenin	6-C- $\alpha$ -L-	-9.515	THR26 (Backbone CO)	2.05
	arabinopyranosyl-8-C- $\beta$ -D-			ASN142 (Side chain CONH <sub>2</sub> )	2.13
	glucopyranoside			HIS163 (Imidazole)	2.32
				GLN189 (Side chain CONH <sub>2</sub> )	2.38
				THR190 (Backbone CO)	2.05



## References

- [1] Zhu H, Wei L, Niu P. The novel coronavirus outbreak in Wuhan, China. *Global Health Research and Policy*. 2020;5:6.
- [2] Khalil A, Tazeddinova D. The upshot of Polyphenolic compounds on immunity amid COVID-19 pandemic and other emerging communicable diseases: An appraisal. *Natural Products and Bioprospecting*. 2020;10:411-29.
- [3] Zuntini AR, Taylor CM, Lohmann LG. Deciphering the Neotropical *Bignonia binata* species complex (Bignoniaceae). *Phytotaxa*. 2015;219:69-77.
- [4] Zuntini AR, Taylor CM, Lohmann LG. Problematic specimens turn out to be two undescribed species of *Bignonia* (Bignoniaceae). *PhytoKeys*. 2015;7.
- [5] Mahmoud BK, Hamed ANE, Samy MN, Kamel MS. Phytochemical and biological overview of genus "Bignonia" (1969-2018). *Journal of Advanced Biomedical and Pharmaceutical Sciences*. 2019;2:83-97.
- [6] Mahmoud BK, Samy MN, Hamed ANE, Abdelmohsen UR, Hajjar D, Yamano Y, Sugimoto S, Matsunami K, Kamel MS. Bignanoside A "A new neolignan glucoside" and bignanoside B "A new iridoid glucoside" from *Bignonia binata* leaves. *Phytochemistry Letters*. 2020;35:200-5.
- [7] Mahmoud BK, Samy MN, Hamed ANE, Desoukey SY, Kamel MS. Anti-infective Activity of *Bignonia binata* Leaves. *Indian Journal of Public Health Research and Development*. 2020;11(4):672-5.
- [8] Samy MN, Hamed ANE, Mahmoud BK, Attia EZ, Abdelmohsen UR, Fawzy MA, Attya ME, Kamel MS. LC-MS based identification of bioactive compounds and hepatoprotective and nephroprotective activities of *Bignonia binata* leaves against carbon tetrachloride induced injury in rats. *Natural Product Research (Formerly Natural Product Letters)*. 2021, Published Online, <https://doi.org/10.1080/14786419.2021.1873982>.
- [9] Johari J, Kianmehr A, Mustafa MR, Abubakar S, Zandi K. Antiviral Activity of Baicalein and Quercetin against the Japanese Encephalitis Virus. *International Journal of Molecular Sciences*. 2012;13:16785-95.
- [10] Vázquez-Calvo A, Jiménez de Oya N, Martín-Acebes MA, García-Moruno E, Saiz JC. Antiviral Properties of the Natural Polyphenols Delphinidin and Epigallocatechin Gallate against the Flaviviruses West Nile Virus, Zika Virus and Dengue Virus. *Frontiers Microbiology*. 2017;8:1314.
- [11] Mahmoud BK, Hamed ANE, Samy MN, Abdelmohsen UR, Attia EZ, Fawzy MA, Refaey RH, Salem MA, Pimentel-Elardo SM, Nodwell J R, Desoukey SY, Kamel MS. Metabolomic profiling and biological investigation of *Tabebuia aurea* (Silva Manso) leaves, family Bignoniaceae. *Natural Product Research (Formerly Natural Product Letters)*, 2019, Published Online, <https://doi.org/10.1080/14786419.2019.1698571>.
- [12] Jin Z, Du X, Xu Y, Deng Y, Liu M, Zhao Y, et al. Structure of M<sup>pro</sup> from SARS-CoV-2 and discovery of its inhibitors. *Nature*. 2020;582:289-93.
- [13] Sarkhail P, Monsef-Esfehani HR, Gholamreza Amin G, Surmaghi MHS, Shafiee A. Phytochemical study of *Phlomis olivieri* Benth. and *Phlomis persica* Boiss. *DARU*. 2006;14(3):115-21.
- [14] Islam MN, Ishita IJ, Jung HA, Choi JS. Vicenin 2 isolated from *Artemisia capillaris* exhibited potent anti-glycation properties. *Food and Chemical Toxicology*. 2014;69:55-62.
- [15] Alwahsh MAA, Khairuddean M, Chong WK. Chemical constituents and antioxidant activity of *Teucrium barbeyanum* Aschers. *Records of Natural Products*. 2015;9(1):159-63.
- [16] Duarte DS, Dolabela MF, Salas CE, Raslan DS, Oliveiras AB, Nenninger A, Wiedemann B, Wagner H, Lombardi J, Lopes MT. Chemical characterization and biological activity of *Macfadyena unguis-cati* (Bignoniaceae). *Journal of Pharmacy and Pharmacology*. 2000;52(3):347-52.
- [17] Aboutabl E., Hashem F. A., Sleem A. and Maamoon A. Flavonoids, anti-inflammatory activity and cytotoxicity of *Macfadyena unguis-cati* L. *African Journal of Traditional, Complementary and Alternative Medicines*. 2008;5(1):18-26.
- [18] Markham KR, Mues R, Stoll M, Zinsmeister HD. NMR spectra of flavone di-C-glycosides from *Apometzgeria pubescens* and the detection of rotational isomerism in 8-C-hexosylflavones. *Zeitschrift für Naturforschung C*. 1987;42(9-10):1039-42.
- [19] Kim MK, Yun KJ, Da Hae Lim JK, Jang YP. Anti-inflammatory properties of flavone di-C-glycosides as active principles of *Camellia mistletoe*, *Korthalsella japonica*. *Biomolecules & Therapeutics*. 2016;24(6):630-7.
- [20] Siewek F, Herrmann K, Grotjahn L, Wray V. Isomeric di-C-glycosylflavones in fig (*Ficus carica* L.). *Zeitschrift für Naturforschung C*. (1985);40(1-2):8-12.
- [21] Xie C, Veitch NC, Houghton PJ, Simmonds MS. Flavone C-Glycosides from *Viola yedoensis* Makino. *Chemical and Pharmaceutical Bulletin*. (2003);51(10):1204-7.
- [22] Abd El-Aziz TM, Stockand JD. Recent progress and challenges in drug development against COVID-19 coronavirus (SARS-CoV-2) - an update on the status. *Infection Genetics and Evolution*. 2020;83:104327.
- [23] Sharma P, Vijayan V, Pant P, Sharma M, Vikram N, Kaur P, Singh TP, Sharma S. Identification of potential drug candidates to combat COVID-19: a structural study using the main protease (mpro) SARS-CoV-2. *Journal of Biomolecular Structure and Dynamics*. 2020;1-11.
- [24] Ahmad A, Kaleem M, Ahmed Z, Shafiq H. Therapeutic potential of flavonoids and their mechanism of action against microbial and viral infections- A review. *Food Research International*. 2015;77:221-35
- [25] Russo M, Moccia S, Spagnuolo C, Tedesco I, Russo GL. Roles of flavonoids against coronavirus infection. *Chemico-Biological Interactions*. 2020;328:109211.
- [26] Nguyen TTH, Woo HJ, Kang HK, Nguyen VD, Kim YM, Kim DW, Ahn SA, Xia Y, Kim D. Flavonoid-mediated inhibition of SARS coronavirus 3C-like protease expressed in *Pichia pastoris*. *Biotechnology Letters*. 2012;34:831-8.